Publishing House
AKAPIT

COMPUTER METHODS IN MATERIALS SCIENCE

Informatyka w Technologii Materiałów

Vol. 7, 2007, No. 1

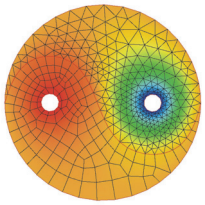

PROBLEM OF THE ARTIFICIAL ANISOTROPY IN SOLIDIFICATION MODELING BY CELLULAR AUTOMATA METHOD

ANDRIY BURBELKO, WOJCIECH KAPTURKIEWICZ, DANIEL GURGUL

AGH University of Science and Technology, Reymonta 23, 30-059 Kraków, Poland

Abstract

Modeling of the dendritic growth by a cellular automaton (CA) can take into account the temperature of the thermodynamic equilibrium as a function of the local concentration and mass diffusion, heat transfer and local temperature, surface energy and curvature of the grain boundaries. Unfortunately, most of the previous solutions produce artificial symmetry of simulation results. This symmetry reflects the anisotropy of the CA computational grid, rather than the properties of the modeled substance. The method of the accuracy ranking estimation for known methods of solidification rate and the interface direction calculation is proposed in the paper. The best solution has been chosen with the highest precision and minimal artificial anisotropy of the simulation results.

Key words: cellular automata, solidification, artificial anisotropy

1. INTRODUCTION

Prediction of the materials microstructure is one of the major tasks of the physical metallurgy. The phase transformation and grain growth modeling by the cellular automata (CA) method is one of the solutions of this problem. In this kind of modeling the grain shapes, internal grain structure and other internal parameters (e.g. dendrite tip radius, secondary dendrite arm space etc.) are estimated at the time of simulation.

The cellular automata are an idealization of a physical system in which space and time are discrete, and the physical quantities take only a finite set of values (Chopard & Droz, 2005). In the solidification modeling the CA apparatus is used for the phase state determination of cell (e.g. "solid", "liquid", "interface"). Known solutions connect the CA simulation of the grain boundary movement and position with the heat and mass transfer problem solution by the finite differences of finite elements methods on the same CA lattice. The review of CA-based models has been presented by Burbelko (2004).

In the case of dendritic growth simulation the main weakness of the most known models is the artificial symmetry and anisotropy: the results of modeling, as noted by Rappaz et al. (1995), reflect the lattice anisotropy rather than properties of modeled substances. The influence of the lattice on the anisotropy during modeling of recrystallization was presented by Kroc (2004, 2005).

The ability of reduction of artificial symmetry is a subject of this paper. The method of the accuracy ranking estimation for known methods of solidification rate and the interface direction calculation is proposed.

2. THE GOVERNING EQUATIONS OF CA MODELING

The details of CA based models for dendrite growth were presented e.g. by Dilthey and Pavlik

 ISSN 1641-8581

(1998), Nastac (1999a), Beltran-Sanchez and Stefanescu (2002, 2003, 2004), and Burbelko (2004). Modeling of the temperature and/or concentration related phase transformation kinetic needs to take into account some physical phenomena, as follow:

– Thermal conductivity

The governing equation for thermal conductivity is the Fourier differential equation with an appropriative primary and boundary condition at the outer border of analyzed domain. In all cells belonging to the phase boundary (interface) the heat source term must be taken into account.

– Component diffusion

The governing equation is the same as for the thermal diffusion (Fourier parabolic partial differential equation). The most popular method of the simulation is the separate solution of this equation in the linear form (without source) at the domains of individual phases or grains: source phase and separate grains of the growing phase. At the phase border the Stefan boundary condition must be taken into account.

– The influence of the segregation and surface curvature on the equilibrium temperature

Linearization of thermodynamic equilibrium system usually is used to take into account the component segregation influence on the equilibrium temperature changes.

The curvature undercooling (a difference between the equilibrium temperature on the plane border and on the curved interface) in two-dimensional space:

$$\Delta T_{\kappa} = \frac{T_m}{L}\left(\sigma + \frac{d^2\sigma}{d\theta^2}\right)\kappa \qquad (1)$$

where: T_m – absolute equilibrium temperature for plane interface, σ – Gibbs surface energy of interface, θ – the angle of the normal vector of the surface with respect to the reference direction, κ – interface curvature.

It was a positive direction of X axis usually used as a reference direction.

– Anisotropy of the interface surface energy

The change of the surface energy with direction is based on the next equation:

$$\sigma(\theta) = \sigma_0\{1 + A_\sigma \cos[m_s(\theta - \theta_0)]\} \qquad (2)$$

where: σ_0 – mean value, A_σ – anisotropy amplitude, m_s – order of crystal symmetry, θ_0 – direction of the preferred crystallographic orientation with a maximal σ value.

– Linear velocity of the interface

The transformation driving force is measured by the difference of the Gibbs energy of interfacial phases. When this value is not too big, it is proportional to the kinetic undercooling ΔT_μ. That is why the expression for growth velocity module is:

$$u = \mu \Delta T_\mu \qquad (3)$$

where μ – kinetic coefficient.

The local kinetic undercooling is obtained from:

$$\Delta T_\mu = T_{Eq}(\mathbf{C}) - T_{Loc} - \Delta T_\kappa \qquad (4)$$

where: T_{Eq} – equilibrium temperature on the plane interface for the local composition $\mathbf{C}$, T_{Loc} – local temperature at the interface.

Growth velocity vector is normal to the surface.

– Kinetic coefficient

The kinetic property of crystal, like the free surface energy, represents an anisotropy. The direction with a lower free surface energy has the larger mobility. Therefore, the following equations for kinetic coefficient are used by Al-Rawahi and Tryggvason (2002):

$$\mu(\theta) = \mu_0\{1 + A_\mu \cos[m_s(\theta - \theta_0)]\}^{-1} \qquad (5)$$

or by Xu (2002):

$$\mu(\theta) = \mu_0\{1 - A_\mu \cos[m_s(\theta - \theta_0)]\} \qquad (6)$$

where μ_0 – mean value and A_μ is an anisotropy amplitude.

– Evolution of solid fraction

Various governing equations for the calculation of the transformation rate are used. Dilthey and Pavlik (1998) estimate the increase in solid fraction, in a time step $\Delta\tau$, from the velocity components u_x and u_y:

$$\Delta f = \frac{\Delta\tau}{a}\left(u_x + u_y - u_x u_y \frac{\Delta\tau}{a}\right) \qquad (7)$$

where a – cell size.

Zhu and Hong (2001) propose the growth length conception:

$$\Delta f = \frac{\Delta\tau}{L} \cdot \frac{u}{\cos\theta_1 + |\sin\theta_1|} \qquad (8)$$

where L – the length of the linking line from the current cell to the nearest neighbor for the current growth direction and θ_1 is the angle between the preferential growth direction of grain with respect to the linking line. The linking line length is $L = a$ if

the growth is directed to the nearest cells and $L = a\sqrt{2}$ if the growth direction is diagonal.

The next equation was proposed by Burbelko (2004) for the evolution of solid phase in rectangular cells:

$$\Delta f = \Delta\tau \frac{u^2}{d_x|u_x| + d_y|u_y|} \tag{9}$$

where d_x, d_y – sizes of rectangular cell.

When the both size of cell are equal, the previous expression may be rearranged to:

$$\Delta f = \frac{\Delta\tau}{a} \frac{u}{|\cos\theta| + |\sin\theta|} \tag{10}$$

As has been developed by Burbelko and Gurgul (2006), one of the reasons of distinct artificial anisotropy of solidification modeling with the CA is above governing equations of the growth rate estimation in the interface cells. For this aim the so-called *stiff circle test* was proposed. The test task is the simulation of the circle grain growth from the nucleus placed in the middle point on a CA lattice with quadratic cells. The direction of velocity vector has been determined on the base of cell coordinates only:

$$\theta = arctg \frac{i - i_N}{j - j_N} \tag{11}$$

where: i, j – an interface cell indexes and i_N, j_N – the nucleus cell indexes.

The components of this vector are

$$u_x = u\cos\theta \quad u_y = u\sin\theta \tag{12}$$

Equations (7), (8) and (10) for growth of solid phase estimation have been tested. Equation (10) gives the best accuracy of estimation of transformed volume in the interface cells. It is seen from figure 1 that equation (7) and (8) introduce distinct artificial anisotropy of growing grains bounds up a CA lattice properties.

– Surface curvature

All known methods of curvature estimation can be classified as: mass or cell counting method (Sasikumar and Sreenivasan, 1994, Dilthey and Pavlik, 1998, Nastac, 1999a), differential (Umancev et al., 1985, Nastac, 1999b) and geometrical (Burbelko, 2004).

According to the mass method, for the same transformed fraction in the current cell, the transformed volume in the surroundings depends on the interface curvature, and expression for curvature estimation is

$$\kappa = \frac{2}{a} \frac{N_{pl} - N_s}{N_t} \tag{13}$$

where: N_{pl} – the number of solid cells in the analyzed surroundings for a planar interface, N_s – the number of solid cells in the analyzed surroundings for a curved interface, N_t – the total number of the cells in the analyzed surrounding.

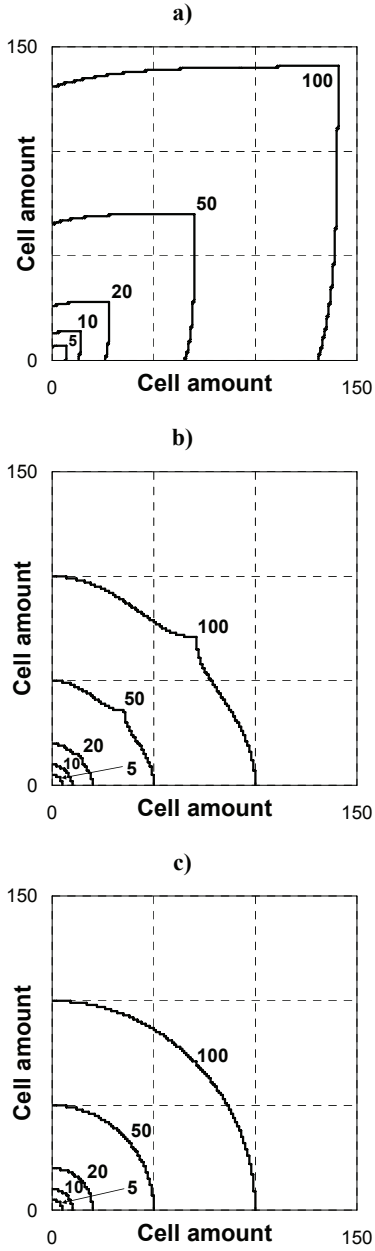

Fig. 1. The grain shapes getting in the stiff circle test (1/4 of perimeter): a) Equation (7); b) Equation (8); c) Equation (10); the numbers near the lines – nominal radii values (Burbelko and Gurgul, 2006).

The differential methods are based on the equations of curvature estimation of lines or surfaces with using of the first and second spatial derivative. When the $y = \varphi(x)$ is an explicit description of the

planar interface line, the curvature of this line is given by (Umancev et al., 1985):

$$\kappa = \frac{\varphi_{xx}}{\left(1+\varphi_x^2\right)^{3/2}} \tag{14}$$

whereas for interface border given by implicit function $F(x,y) = \text{const}$, the curvature is calculated as (Nastac, 1999a):

$$\kappa = \frac{2F_{xy}F_xF_y - F_{xx}F_y^2 - F_{yy}F_x^2}{\left(F_x^2+F_y^2\right)^{3/2}} \tag{15}$$

where the low indexes mean the differentiation with respect to appropriative value.

The geometrical method is based on the geometry definition of a planar curve as a limit of the ratio of the change in the angle of a tangent that moves over a given arc to the length of the arc as the length of the arc approaches zero:

$$\kappa \approx \frac{\Delta\theta}{\Delta s} \tag{16}$$

where: $\Delta\theta$ – the angle between the unit normal vectors in the adjacent interface cells, Δs – the front length.

3. THE GOVERNING EQUATIONS FOR SURFACE ORIENTATION (GROWTH DIRECTION)

In our opinion, the directly linking of interface orientation with a temperature or concentration (Nastac, 1999b; Beltran-Sanchez and Stefanescu, 2002) gradient has a worse precision in comparison with a determination of surface normal vector from the spatial distribution of solid phase.

The definition of interface orientation using so-called **F** vector is proposed by Dilthey and Pavlik (1998). The value of this vector is equal to the total amount of solid fraction within a circle area with radius R. The vector of surface orientation being along the line connecting the center of mass of the total solid and the center of the regarded cell. The interface normal vector can be worked out by:

$$\mathbf{n} = -\left(\sum_j \mathbf{r}_j f_j\right) \Bigg/ \left[\left(\sum_j x_j f_j\right)^2 + \left(\sum_j y_j f_j\right)^2\right]^{1/2} \tag{17}$$

where: $\mathbf{r}_j$ – radius-vector from the current cell to the j cell, f_j – solid fraction in the j cell, x_j, y_j – the vector $\mathbf{r}_j$ components.

The angle of this vector with respect to the reference direction of X axis is:

$$\theta = \arctan\left(\sum_j y_j f_j \Big/ \sum_j x_j f_j\right) \tag{18}$$

Another method of the interface direction estimation used by Beltran-Sanchez and Stefanescu (2003, 2004) is based on the concept that the interface direction is equal to the gradient of f-field (transformed volume fraction f changes from 0 to 1 in the area of interface cell with fragments of two neighbor cells). The angle of the gradient vector with respect to the reference direction of X axis is defined as:

$$\theta = \arctan\left(\frac{\mathrm{d}f}{\mathrm{d}y} \Big/ \frac{\mathrm{d}f}{\mathrm{d}x}\right) \tag{19}$$

The implementations of the equations (18) and (19) for different neighboring are similar:

$$\theta = \arctan\left(\sum A_j f_j \Big/ \sum B_j f_j\right) \tag{20}$$

where A_j and B_j – coefficients dependent on a calculation method and neighborhood size.

Hence, there were different solutions known for the problems of transformed volume evolution, growth direction and front curvature. The test method for objective appraisal of the governing equation for transformed volume evolution has been developed by Burbelko and Gurgul (2006).

Unfortunately, the objective appraisal of the methods of growth direction and front curvature calculation is still unknown. Below we will present an evaluation method of the equations used for calculation of growth direction.

4. TESTING OF THE GROWTH DIRECTION GOVERNING EQUATIONS

The test task is the simulation of the circle grain growth from the nucleus placed in the middle point on a CA lattice with quadratic cells. The initial solid fraction in the nucleus cell is $f_0 = 1$. The direction of velocity vector (θ) has been determined on the base of testing equations. Next, the components of the interface velocity vector are calculated with equation (12) and evolution of the solid fraction in the interface cells with equation (10). This task has been named as *weak circle test*.

The equations (18) and (19) have been tested with a few neighborhood sizes (4, 8, 12, 20 and 24 cells). The implementation of these equations for tested neighborhood radii is presented in table 1. When the neighborhood radius is equal to a (4-cell surround-

ings) or $a\sqrt{2}$ (8-cell surroundings), the implementations of both these equations are the same.

Table 1. *The tested equations for growth direction estimation.*

Radii (Amount of cells)	Equation	Implementation: tan θ =	Index
a (4)	(18), (19)	$=\frac{f_{0,1}-f_{0,-1}}{f_{-1,0}-f_{1,0}}$	A
$a\sqrt{2}$ (8)	(18), (19)	$=\frac{f_{-1,1}+f_{0,1}+f_{1,1}-f_{-1,-1}-f_{0,-1}-f_{1,-1}}{f_{1,1}+f_{1,0}+f_{1,-1}-f_{-1,1}-f_{-1,0}-f_{-1,-1}}$	B
$2a$ (12)	(18)	$=\frac{2\left(f_{0,2}-f_{0,-2}\right)+f_{-1,1}+f_{0,1}+f_{1,1}-f_{-1,-1}-f_{0,-1}-f_{1,-1}}{2\left(f_{2,0}-f_{-2,0}\right)+f_{1,1}+f_{1,0}+f_{1,-1}-f_{-1,1}-f_{-1,0}-f_{-1,-1}}$	C
$2a$ (12)	(19)	$=\frac{f_{0,2}+f_{-1,1}+f_{0,1}+f_{1,1}-f_{-1,-1}-f_{0,-1}-f_{1,-1}-f_{0,-2}}{f_{2,0}+f_{1,1}+f_{1,0}+f_{1,-1}-f_{-1,1}-f_{-1,0}-f_{-1,-1}-f_{-2,0}}$	D
$a\sqrt{5}$ (20)	(18)	$=\frac{\left[\begin{array}{l}2\left(f_{-1,2}+f_{0,2}+f_{1,2}-f_{-1,-2}-f_{0,-2}-f_{1,-2}\right)+f_{-2,1}+f_{-1,1}+\\+f_{0,1}+f_{1,1}+f_{2,1}-f_{-2,-1}-f_{-1,-1}-f_{0,-1}-f_{1,-1}-f_{2,-1}\end{array}\right]}{\left[\begin{array}{l}2\left(f_{2,1}+f_{2,0}+f_{2,-1}-f_{-2,1}-f_{-2,0}-f_{-2,-1}\right)+f_{1,2}+f_{1,1}+\\+f_{1,0}+f_{1,-1}+f_{1,-2}-f_{-1,2}-f_{-1,1}-f_{-1,0}-f_{-1,-1}-f_{-1,-2}\end{array}\right]}$	E
$a\sqrt{5}$ (20)	(19)	$=\frac{\left(\begin{array}{l}f_{-1,2}+f_{0,2}+f_{1,2}-f_{-1,-2}-f_{0,-2}-f_{1,-2}+f_{-2,1}+f_{-1,1}+\\+f_{0,1}+f_{1,1}+f_{2,1}-f_{-2,-1}-f_{-1,-1}-f_{0,-1}-f_{1,-1}-f_{2,-1}\end{array}\right)}{\left(\begin{array}{l}f_{2,1}+f_{2,0}+f_{2,-1}-f_{-2,1}-f_{-2,0}-f_{-2,-1}+f_{1,2}+f_{1,1}+\\+f_{1,0}+f_{1,-1}+f_{1,-2}-f_{-1,2}-f_{-1,1}-f_{-1,0}-f_{-1,-1}-f_{-1,-2}\end{array}\right)}$	F
$2a\sqrt{2}$ (24)	(18)	$=\frac{\left[\begin{array}{l}2\left(f_{-2,2}+f_{-1,2}+f_{0,2}+f_{1,2}+f_{2,2}-f_{-2,-2}-f_{-1,-2}-f_{0,-2}-f_{1,-2}-f_{2,-2}\right)+\\+f_{-2,1}+f_{-1,1}+f_{0,1}+f_{1,1}+f_{2,1}-f_{-2,-1}-f_{-1,-1}-f_{0,-1}-f_{1,-1}-f_{2,-1}\end{array}\right]}{\left[\begin{array}{l}2\left(f_{2,2}+f_{2,1}+f_{2,0}+f_{2,-1}+f_{2,-2}-f_{-2,2}-f_{-2,1}-f_{-2,0}-f_{-2,-1}-f_{-2,-2}\right)+\\+f_{1,2}+f_{1,1}+f_{1,0}+f_{1,-1}+f_{1,-2}-f_{-1,2}-f_{-1,1}-f_{-1,0}-f_{-1,-1}-f_{-1,-2}\end{array}\right]}$	G
$2a\sqrt{2}$ (24)	(19)	$=\frac{\left(\begin{array}{l}f_{-2,2}+f_{-1,2}+f_{0,2}+f_{1,2}+f_{2,2}-f_{-2,-2}-f_{-1,-2}-f_{0,-2}-f_{1,-2}-f_{2,-2}+\\+f_{-2,1}+f_{-1,1}+f_{0,1}+f_{1,1}+f_{2,1}-f_{-2,-1}-f_{-1,-1}-f_{0,-1}-f_{1,-1}-f_{2,-1}\end{array}\right)}{\left(\begin{array}{l}f_{2,2}+f_{2,1}+f_{2,0}+f_{2,-1}+f_{2,-2}-f_{-2,2}-f_{-2,1}-f_{-2,0}-f_{-2,-1}-f_{-2,-2}+\\+f_{1,2}+f_{1,1}+f_{1,0}+f_{1,-1}+f_{1,-2}-f_{-1,2}-f_{-1,1}-f_{-1,0}-f_{-1,-1}-f_{-1,-2}\end{array}\right)}$	H

Deviation of the grain interface direction calculated by above equations leads to the divergence between the simulated grain shapes and shape of the grain obtained in the *stiff circle test*, presented in figure 1c. The results of the *weak circle test* are plotted in figure 2. It is clear that the governing equation for interface direction estimation may be the source of the artificial anisotropy of simulation results connected with a CA lattice anisotropy. The minimal distortion gives the equation E, table 1 (implementation of equation (18) for the surroundings of a $a\sqrt{5}$ radius and 20 cells neighborhood).

The quantitative rating of tested equations was calculated. The radius-vector length of interface for each interface cell is

$$R_{i,j}=\sqrt{\left(i-i_N\right)^2+\left(j-j_N\right)^2}+f_{i,j}-0.5 \qquad (21)$$

For the perfect solution the nominal grain radius should increase from 1 to 101 lattice spacing in the test condition. The tests results in the quantitative form are presented in table 2. There are the next precision marks of the tested equations: differences between minimal, maximal and mean value of radius obtained in testing and the appropriate value obtained in the *stiff circle test*. The quantitative rating presented in the table 2 is consistent with figure 2. The implementation E (table 2) gives the best precision of the grain radius estimation (the minimal

standard deviation of relative radius 0.24 in comparison with 0.13 in the *stiff circle test*). In this case the divergence of the grain interface direction from theoretical one is no higher then 2.6°. It is the minimal value of direction error for all tested equations. This equation provides to the most homogeneous results (as it is illustrated in figure 2e) and to the minimal standard deviation of direction divergence equal to 0.64°.

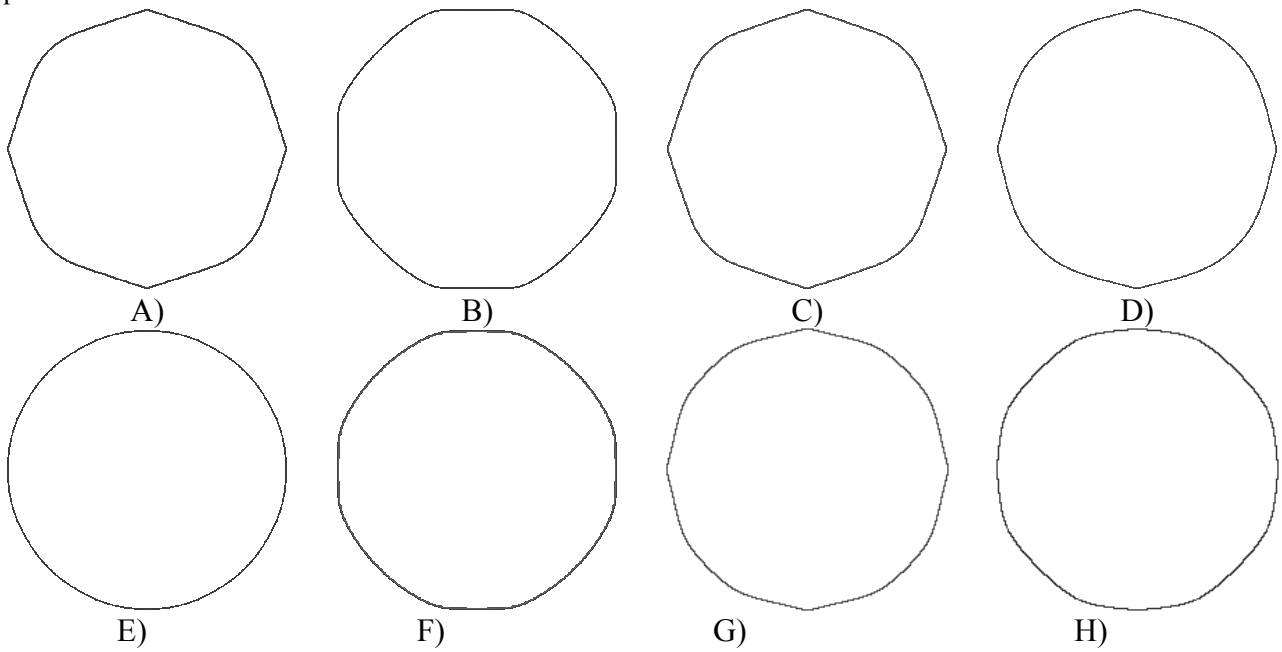

Fig. 2. *The grain shapes obtained in the weak circle test of the growth direction governing equations (implementations – see table 1).*

Table 2. *The results of the test of the surface direction governing equations.*

Test	Radii (R/a)			Radius standard deviation (σ/a)	Angle divergence (deg.)	
	min	max	mean		max	standard deviation
base values – stiff circle test						
	100.4	101.0	100.8	0.13	–	–
weak circle test						
A	96.0	101.0	98.2	1.60	24.7	7.23
B	100.4	104.6	102.2	1.28	13.1	3.50
C	96.1	101.0	98.2	1.57	24.1	7.06
D	97.9	101.0	99.4	0.93	15.2	4.30
E	**100.3**	**101.1**	**100.7**	**0.24**	**2.6**	**0.64**
F	100.4	103.2	101.7	0.84	8.4	2.27
G	98.6	101.1	100.0	0.85	12.7	3.28
H	100.4	102.9	101.5	0.73	6.4	1.87

For the E and G cases (equation 18, table 2) for the larger neighborhood the worse accuracy is obtained. The results of equation (19) are better for 24-cells neighborhood (case H) then for 20-cells one (case F), but precision of this equation is still worse then for case E. From the above calculations is visible that the obvious influence of larger neighborhood is not clear-cut.

5. CONCLUSIONS

The source of artificial anisotropy of solidification modeling by the CA can be governing equations of the solidification rate and the interface direction calculation.

The *weak circle test* is proposed for the verification of the growth direction governing equations in solidification modeling by cellular automata method.

The equation E in table 1 gives the maximal precision of growth direction estimation and produces the minimal anisotropy of simulation results.

Acknowledgements. This paper was supported by Polish Ministry of Education and Science (Project N507 071 31/1623)

REFERENCES

Al-Rawahi, N., Tryggvason, G., 2002, Numerical simulation of dendritic solidification with convection: two-dimensional geometry, *J. of Comp. Physics*, 180, 471–496.

Beltran-Sanchez, L., Stefanescu, D.M., 2004, A quantitative dendrite growth model and analysis of stability concepts, *Metall. and Materials Trans*., A, 35A, 2471–2485.

Beltran-Sanchez, L., Stefanescu, D.M., 2002, Growth of solutal dendrites. A cellular automaton model, *Int. Journ. of Cast Metals Res*., 15, 251–256.

Beltran-Sanchez, L., Stefanescu, D.M., 2003, Growth of solutal dendrites: a cellular automaton model and its quantitative capabilities, *Metall. and Materials Trans. A*, 34A, 367–382.

Burbelko, A., 2004, *Mezomodelowanie krystalizacji metodą automatu komórkowego*, Uczeln. Wydawm. N.-D. AGH,

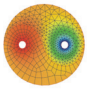

Kraków (in Polish).
Burbelko, A.A., Gurgul D., 2006, Testing of the Growth Rate Governing Equations for Cellular Automata Solidification Modeling, *Simulation, Design and Control of Foundry Processes*, AGH, Kraków, 21-32.
Chopard, B., Droz, M., 2005, *Cellular automata modeling of physical systems*, University Press, Cambridge.
Dilthey, U., Pavlik, V., Reichel, T., 1997, Numerical simulation of dendritic solidification with modified cellular automata, *Mathematical Modelling of Weld Phenomena – 3*, eds, Cejrak H., Bhadeshia H.K.D.H., The Institute of Materials, London, 85-105.
Dilthey, U., Pavlik, V., 1998, Numerical simulation of dendrite morphology and grain growth with modified cellular automata, *Modeling of* Casting, *Welding and Advanced Solidification Processes VIII. TMS*, Warrendale, 589–596.
Kroc, J., 2004, Effect of Lattice Anisotropy on Simulations of Grain Boundary Movement in Two-dimensions, *Materials Science Forum*, 467-470, 1069-1074.
Kroc, J., 2005, Influence of Lattice Anisotropy on Models Formulated by Cellular Automata in Presence of Grain Boundary Movement: A Case Study, *Materials Science Forum*, 482, 195-198.
Nastac, L., 1999a, Numerical modeling of solidification morphologies and segregation patterns in cast dendritic alloys, *Acta Mater*., 47, 4253–4262.
Nastac, L., 1999b, Solidification structure modeling in ingots processed through primary and secondary remelt operations, *Int. J. of Cast Metals Res*., 15, 279–284.
Rappaz, M., Gandin, Ch.-A., Jacot, A., Charbon, Ch., 1995, Modeling of microstructure formation, *Modeling of Casting, Welding and Advanced Solidification Processes –VII*, eds, Cross, M., Campbell, J., TMS, Warrendale, 501–516.
Sasikumar, R., Sreenivasan, R., 1994, Two Dimensional Simulation of Dendrite Morphology, *Acta Metall. Mater*, 42, 2381-2386.
Umancev, R.A., Vinogradov, V.V., Borisov, V.T., 1985, Metematićeskoje modelirovanieje rosta dendritov v pereohlazhdennom rasplave, *Kristallografija*, 30, 455-460 (in Russian).
Xu, J.-J., 2002, Stability and selection of dendritic growth with anisotropic kinetic attachment, *J. Cryst. Growth*, 245, 134-148.
Zhu, M.F., Hong, C.P., 2001, A modified cellular automation model for the simulation of dendritic growth in solidification of alloys. *ISIJ Int.*, 41, 436–445.

PROBLEM SZTUCZNEJ ANIZOTROPII W MODELOWANIU KRYSTALIZACJI Z WYKORZYSTANIEM AUTOMATÓW KOMÓRKOWYCH

Streszczenie

Modelowanie krystalizacji ziaren dendrytycznych z wykorzystaniem automatów komórkowych (AK) pozwala uwzględnić szereg zjawisk: zmianę temperatury równowagi termodynamicznej na granicy faz pod wpływem zmiany lokalnego składu chemicznego w wyniku redystrybucji i dyfuzji składników, przepływ ciepła, wpływ krzywizny granicy międzyfazowej i jej energii powierzchniowej. Niestety, większość ze znanych dotychczas rozwiązań generuje sztuczną symetrię wyników modelowania, która odzwierciedla w większym stopniu anizotropię stosowanej siatki obliczeniowej, aniżeli właściwości modelowanych substancji. W pracy udowodniono, że przyczyny sztucznej symetrii mają związek ze stosowanymi metodami obliczenia szybkości przemiany fazowej i kierunku migracji granicy międzyfazowej. Przedstawiono sposób wyznaczania ocen dokładności tych metod. Na postawie opracowanej procedury oceny wybrano metody i równania, zapewniające najwyższą precyzję i minimalny poziom sztucznej anizotropii wyników modelowania.

Submitted: November 3, 2006
Submitted in a revised form: November 14, 2006
Accepted: December 1, 2006